Version_0.53 from 03.03.2003
Last change: 20.12.2003

IBH - Ingenieurbüro
Dr.-Ing. Michael Herdy

Introductory Theory Manual

ViscoData & ViscoShift

(Preliminary Version)

Contents

1) Preface

In the present edition, a software, called ViscoData, is described. It allows the user to create a PRONY series from dynamic modulus data as well as from relaxation data. Furthermore it is described a so called pre-processor, named ViscoShift which prepares the measured isotherm data to create a master curve by appropriate shifting individual isotherms, resulted by DMA or relaxation measurements, respectively. Use of this software is illustrated by means of examples, which the user can follow along at his own computer screen.

2) Introduction

The first chapter of this handbook comprises an abbreviated text on the general subject of polymer and elastomer viscoelasticity. It is intended as a refresher on terminology and concepts, primarily for those already conversant with the methods. However, various references are provided for those interested in a greater depth of detail [1,2,3,4].

In chapter 4 the software ViscoData and ViscoShift is introduced by means of examples. The greatest value of the software system described in this handbook is a quick and liable determination of the parameters of discrete relaxation spectra of rubbers and plastics in the first place, but also for other materials. The parameters of the resulted spectra are often expressed in the form of a Prony series. The goal of being able to predict the stress-strain-temperature response of elastomers is a difficult one because of the complex thermo-mechanical behavior elastomers exhibit. In fact to a large degree the tremendous utility of elastomer materials is based on this complexity and the fact that the material properties can change drastically over a relative narrow time or temperature span**.**

3) Dynamic mechanical properties of polymers / elastomers

3.1 General remarks

Often polymers, including elastomers, are considered mainly as an ideal elastic body with ideal behaviour. That is to say, it is often assumed that reversible relations between load and displacement exist. In practice however, deviations from such ideal elastic behaviour are to be expected. In this section we shall consider the measurement and interpretation of these deviations. Here we will focus on elastomers, but most of the facts considered in the following are also valid for plastics and in some sense even for metals. Rubbery materials (another notation is "elastomers") combine properties of both solids and liquids. For example they show some viscose behaviour. For example "strain-rate strengthening" and relaxation are two manifestations of the viscose properties of such

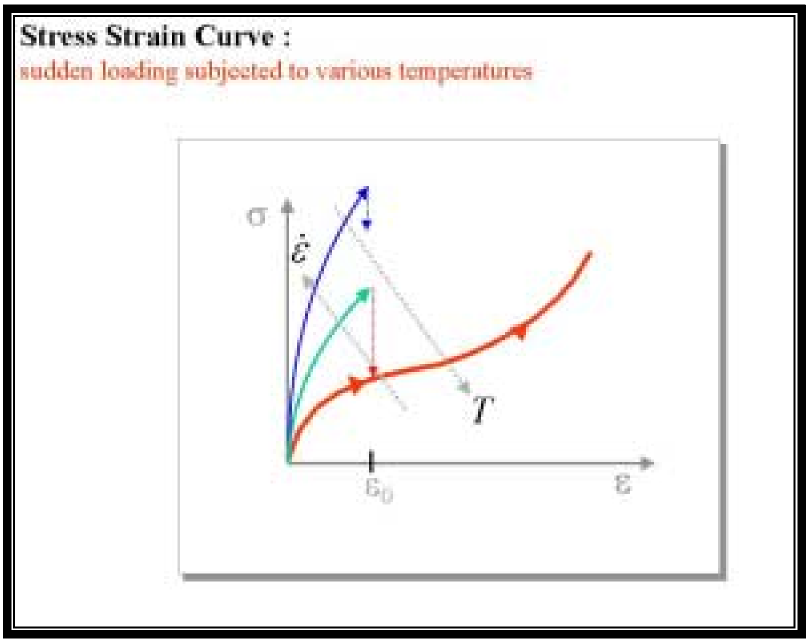

Fig.3.1: "Strain-hardening" by rapid deformation under high and low temperatures (schematised curves). Stress-strain curves become steeper the higher the strain rate and/or the lower the temperature. The lower red curve represents the equilibrium stress-strain curve, where the strain rate tends to go to zero, while the temperature is sufficiently high. The arrows shown on the straight lines indicate the direction of increase for the respective quantities T and $\dot{\varepsilon}$ ($\dot{\varepsilon}$ represents the rate of strain and T gives the temperature).When the sample is strained to a certain value and then held constant

stress starts to relax until the equilibrium value is approached. The time to reach that value is bigger the lower the temperature.

materials***. Fig.3.1*** shows the effect of “strain-hardening” under rapid straining under various temperature conditions. In general a broad range of temperatures has to be considered as well as various loading rates in order to be able to extract the wanted viscoelastic informations from the material in question. .

The term “dynamic mechanical properties” DMP (measured by a Dynamic Mechanical Analyser DMA) refers to the behaviour of elastomers when subjected to stresses or strains that change with time. For example in creep experiments one measures the increase in strain with time, the stress being held constant, whereas in stress relaxation experiments one measures the decrease in stress with time under constant strain conditions (see also ***Fig.3.2*** *for the relaxation type*). Usually, the elasticity is represented by a spring, while the viscosity is given by a dash pot (a piston which moves in a cylinder filled with a viscous fluid) which follows the Newtonean law. The simplest model of a visco-elastic body is therefore a combination of a spring and a dash pot either in a parallel or in a serial arrangement. The former is called the Kelvin-Voigt model and the latter is called the Maxwell model. Both models exhibit in principle visco-elastic behavior. The Maxwell model is capable to describe stress relaxation, while the Kelvin-Voigt model is suitable for the description of strain retardation. Both exhibit a phase-shift when applied for a dynamical experiment. The proportion of the viscosity of the dash pot to the spring rate is called the retardation time constant in case of Kelvin-Voigt model and relaxation time constant when referred to the Maxwell model. If one has to describe in a constitutive model not only the strain retardation but also the stress relaxation, one is led to the so called three-parameter model or often called the Standard Model of Visco-Elasticity (see Fig.3.2) . This model contains in principle two Maxwell elements in parallel. One of the two (left one) “dash pots” possesses a viscosity which can be considered tending to go to infinity. That restriction prevents yielding of the material in the long term and ensures to have a real solid body. It further turns out that this model contains two characteristic time constants, namely a relaxation time as well as a retardation time constant, respectively to consider both relaxation as well as retardation processes in one single model. Under a constant strain ε_0 the resulting stress is decaying with time as is shown in Fig.3.2.

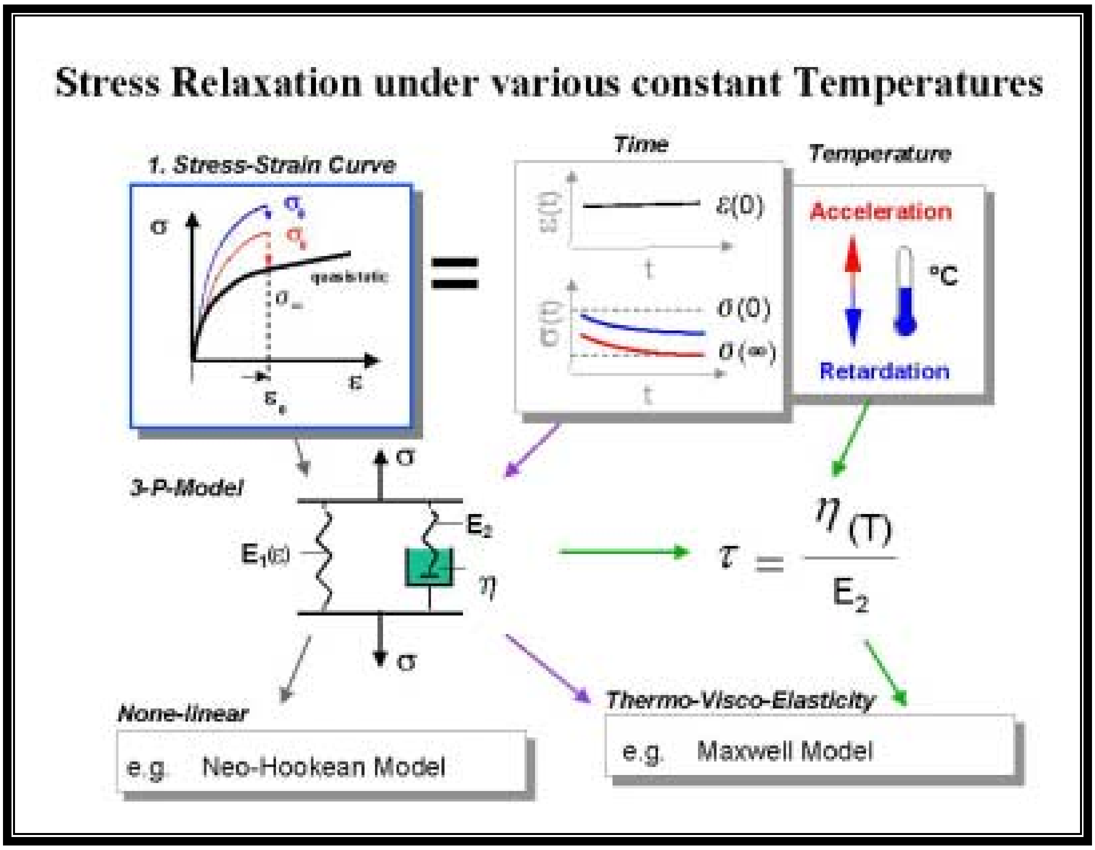

Fig.3.2: Stress relaxation as one of the various types of thermo-visco-elastic experiments. The standard model of viscoelasticity is suitable for strain retardation and stress relaxation as well. The three-parameter Standard-Model of Viscoelasticty is shown to describe proper stress relaxation for a solid body. Also the dependence of temperature on the stress relaxation time constant can be described in the vicinity of that model.

In the following we shall also discuss the special case of sinusoidally varying stresses and strains often used in DMA measurements. An oscillatory dynamic experiment differs from simple creep and stress relaxation studies in two important respects. The time scale is determined (inversely) by the frequency of the sinusoidal deformation. Second, stress and strain are not in phase in a dynamic experiment.

The main cause of delayed elastic response in rubbery solids is “internal viscosity” between molecular chains. This property is strongly affected by temperature and the measure is usually given by the relaxation time τ. It depends on the rate at which small segments of a molecule move to new positions as a result of random Brownian motion. The value of τ decreases strongly with increasing temperature as is shown and motivated in ***Fig.3.2***. The dependence of τ on temperature follows a characteristic law (see later ....).

At temperatureT_g molecular segments move so slowly, about once in one second, that for practical purposes they do not move at all and the material becomes a rigid glass. The temperature $\mathrm{T_g}$ is denoted the glass transition temperature. It is the single most important parameter determining low temperature response of an elastomer. For example, for cushioning a pressure impact, we require virtually complete rubberlike response in the time of pressure pulse duration of the order of several micro-seconds. But molecular segments will move in 1 ms only when a molecule segment can jump 1000 times per second: i.e., only at a temperature about 15°C higher than $\mathrm{T_g}$. Indeed, for co-ordinated motion of entire molecular strands, consisting of many segments, to take place within 1 ms, the segmental response frequency must be still higher, by a factor 100 or so. This rapidity of response is achieved only at a temperature about 30°C above $\mathrm{T_g}$. Thus, we do not expect rapid, fully rubbery response until temperatures of more than $\mathrm{T_g}$ +30°C are attained.

3.2. Visco-elastic equation of state

The response of a material to an applied strain and temperature can, in principle, be predicted if the viscoelastic equation of state is known.

The three-parameter Maxwell model (often called the standard model of viscoelasticity, see also ***Fig.3.2***) is useful in describing the viscoelastic response of amorphous high polymers to which elastomers belong. This model shows all the properties which can be observed for the mentioned materials at least qualitatively. Quantitatively, the model is able to describe the observed properties only over a small region of temperature and/or time scale. However, engineers are very often interested in a broad range of time and temperature, and indeed experimental studies of amorphous polymers, respectively elastomers, clearly show that the viscoelastic response generally cannot be quantitatively represented by a three-parameter Maxwell model. In addition to an instantaneous elastic response, elastomers in general possess a series of relaxation mechanisms which respond to an applied strain and temperature. Therefore a multiplicity of Maxwell elements in parallel is needed in order to accurately model the stress-strain behaviour of elastomers (rubbery materials) over a broad range of temperature and time. This leads to the generation of a spectrum of Maxwell elements of various relaxation strength and relaxation time constants. The following sub-chapter will discuss accepted practices [8] for obtaining the necessary data for generating the respective so called relaxation spectra (Prony series).

3.3 Time-temperature superposition principle

The simplest way to characterise the elastic properties of an elastomer is to measure its modulus of elasticity as a function of temperature. The modulus of an elastomer at a given strain level, however, is a function of time as well as a function of temperature. A convenient and appropriate way to completely describe this dual functionality is by using time-temperature superposition to generate master curves and shift factors. The time-temperature superposition principle states that the viscoelastic behavior at one temperature can be related to that at another temperature by a change in time scale [1]. Mathematically this idea can be expressed as:

$$E(T_1,t)=E\left(T_2,\frac{t}{a_T}\right)\cdot\frac{\rho(T_1)T_1}{\rho(T_2)T_2} \quad ,$$

where the effect of changing temperature is the same as applying a horizontal displacement of, ***lg*** $\boldsymbol{a_T}$, on a log-log plot of modulus ***E*** vs. time ***t*** . The above equation defines two shift-factors $\boldsymbol{a_T}$ and $\boldsymbol{b_T}$, respectively, where the former one can be determined directly from experimental relaxation curves as shown in ***Fig.3.3*** . The quotient $\rho(T_1)T_1/(\rho(T_2)T_2)=b_T$ is an inherent correction factor (vertical shift factor) for the change in the modulus due to a change in temperature. According to the theory of rubber elasticity [5], this correction factor changes slightly with temperature compared with the large change due to accompanied horizontal shift $\boldsymbol{a_T}$. Thus it is usually sufficient to apply a horizontal shift on the time scale only.

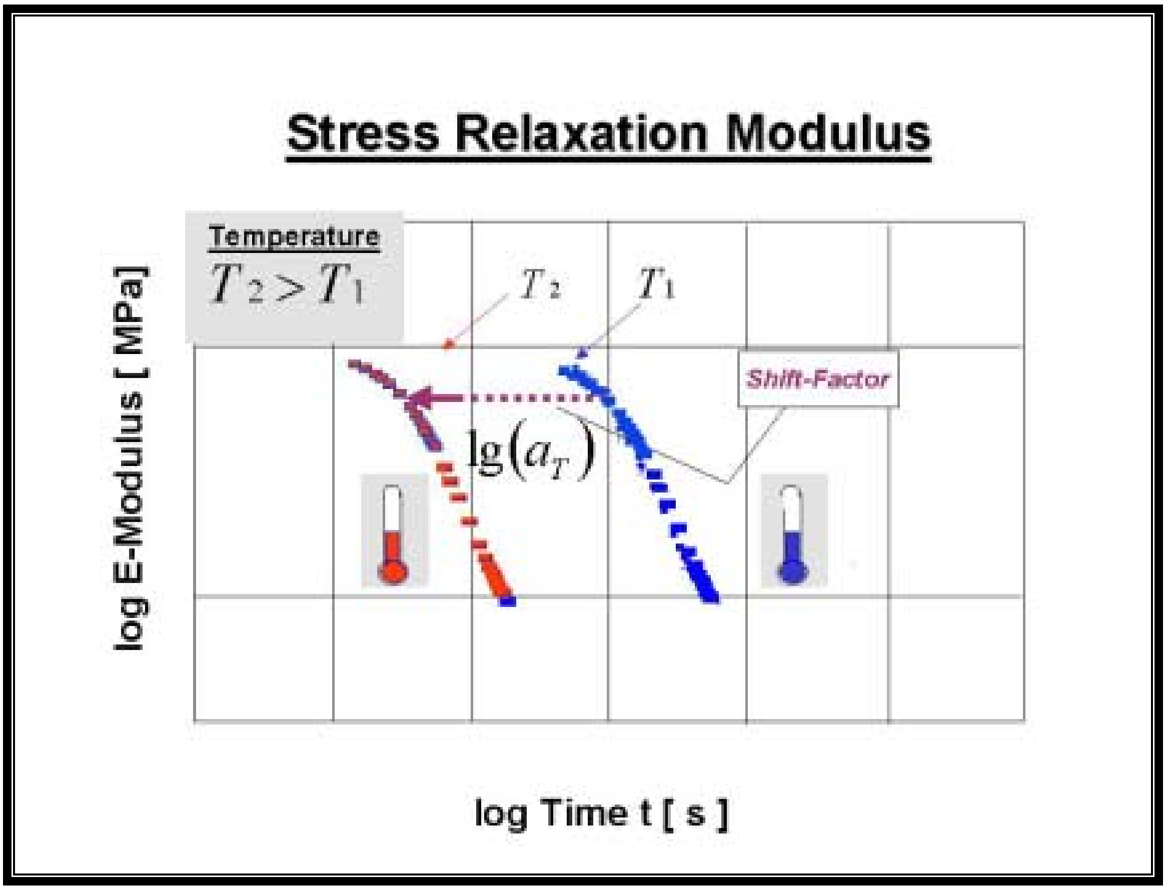

Fig. 3.3: Stress relaxation modulus data taken at two different temperatures T_1 and T_2 and plotted against ***log t*** show that the shapes of the curves are the same and therefore are superimposed by using a "shift" factor ($\lg a_T$) .

3.4. Shift-Equations

A significant observation, established by the work of Williams, Landel and Ferry [6], is that for the transition from the rubbery to the glassy state for many amorphous polymers the dependence of the shift-factor on temperature follows the same general relationship. It was found that:

$$\lg\ a_T = \frac{c_1(T - T_g)}{c_2 + T - T_g} \quad ,$$

where c_1 and c_2 are constants, and T_g is the glass transition temperature. This relation holds around the glass transition temperature (approx. ± 15°C) and sometimes (... it varies from elastomer to elastomer) it is also valid for higher temperatures - but never valid for lower temperatures. Knowing a_T, one can compute the relaxation time at any temperature from the equation

$$\tau(T) = a_T \tau(T_g) \quad ,$$

where $\tau(T_g)$ is the relaxation time at glass transition temperature $\boldsymbol{T_g}$.

3.5. Stress relaxation modulus

In a stress relaxation experiment, the stress at a constant strain is determined as a function of time after a sudden imposition of the strain. The stress may decay either to an equilibrium value or to zero, depending on the structure of the material (in case of a cross-linked rubber the stress will approach an equilibrium value, depending on the degree of cross-linking).

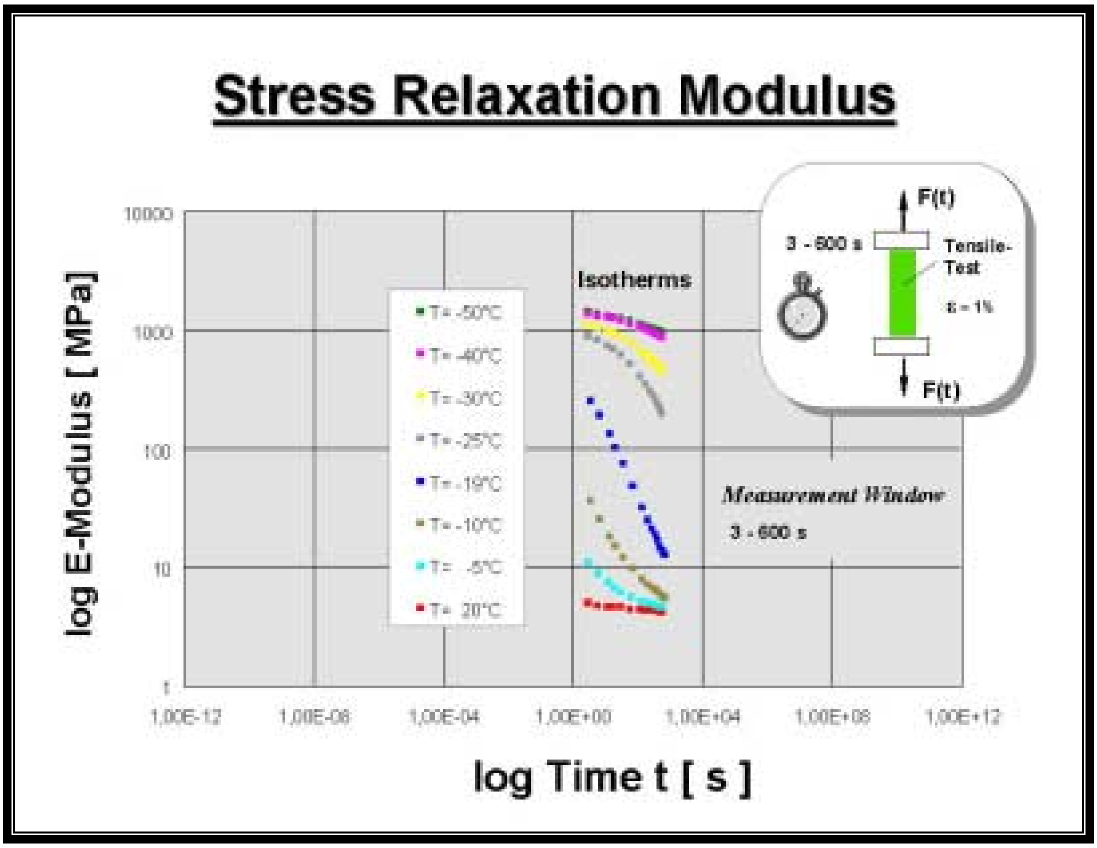

Fig.3.4: A typical plot of stress relaxation curves in a log-log diagram resulting from a strain of 1% in tension, measured in a “time-window” of 3sec<t<600sec for various temperatures is shown [7,8].

An example of stress relaxation data is shown in ***Fig. 3.4***, taken from a work of Ajroldi and co-workers [7] on a fluoro-carbon rubber with a 75 Shore A hardness. This type of test typically delivers the relaxation modulus as a function of time ***t*** at constant temperature ***T***. The curves shown result from an applied strain in tension (1% elongation), measured in a time span of : 3sec. < ***t*** < 600sec. for various temperatures (9 isotherms). The glass transition temperature T_g was ***–19°C***, whereby the corresponding stress relaxation isotherm is marked by a dark-blue color in ***Fig. 3.4.*** It is interesting to observe that this curve shows the strongest decay in stress during the measurement compared with the other ones. Stress relaxation isotherms well below this temperature represent an “organic glass” and possess a modulus in the order of magnitude of 10^3 MPa. On the other side, for isotherms well above the glass transition temperature, the elastomer represents a rubbery elastic solid with a modulus in the order of magnitude of several MPa.

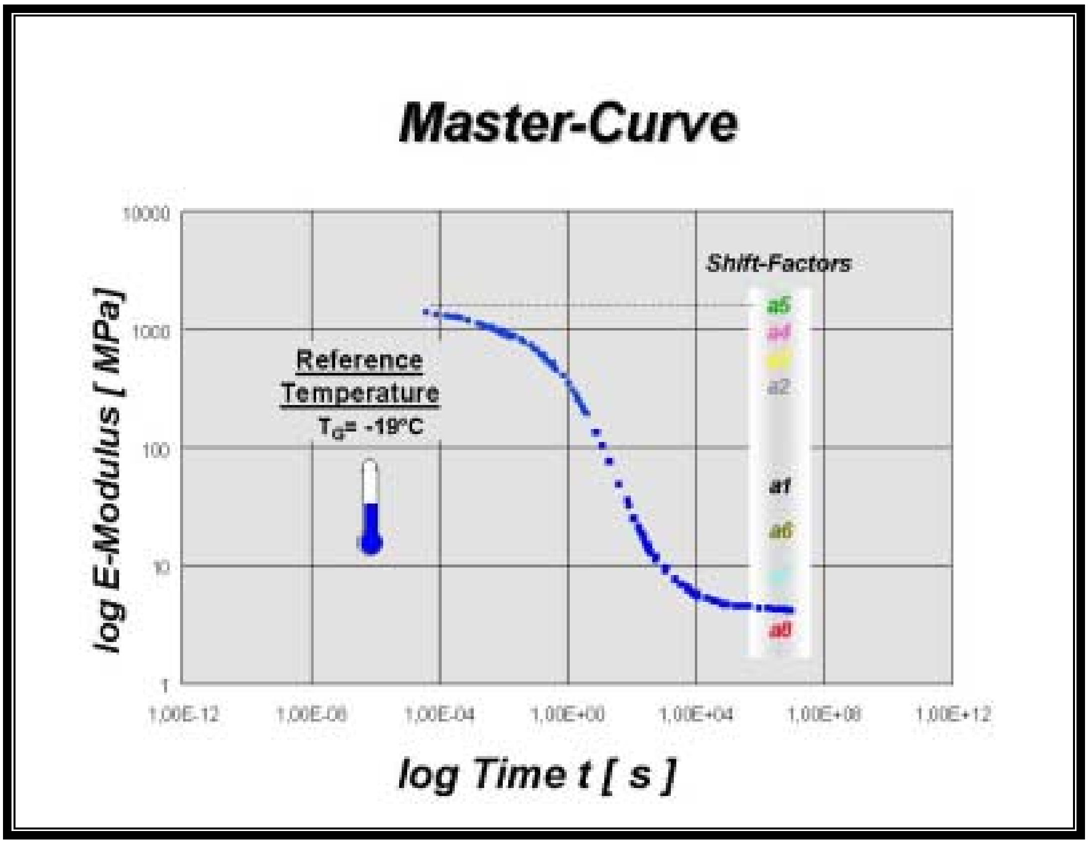

Fig.3.5 Construction of a master curve (see also Fig.3.4 from which that master curve has been constructed). The resulted curve represents a singular isotherm for the temperature $T = T_G = -19^\circ C$. But this time for an extended time span compared to the ‘experimental time window’ of each isotherm (see also Fig.3.4 for comparison).

The time-temperature superposition principle states that the given series of time dependent stress relaxation isotherms can be superimposed to produce a single isotherm by horizontal shifts along the time axis. It is thus assumed, as already mentioned above, that the general effect of temperature on an elastomer is to multiply all relaxation times by a factor, which is defined by the resulted experimental shift factor itself. Thus in the present case the time-temperature superposition principle was applied to construct the stress relaxation master curve shown in ***Fig. 3.5***.

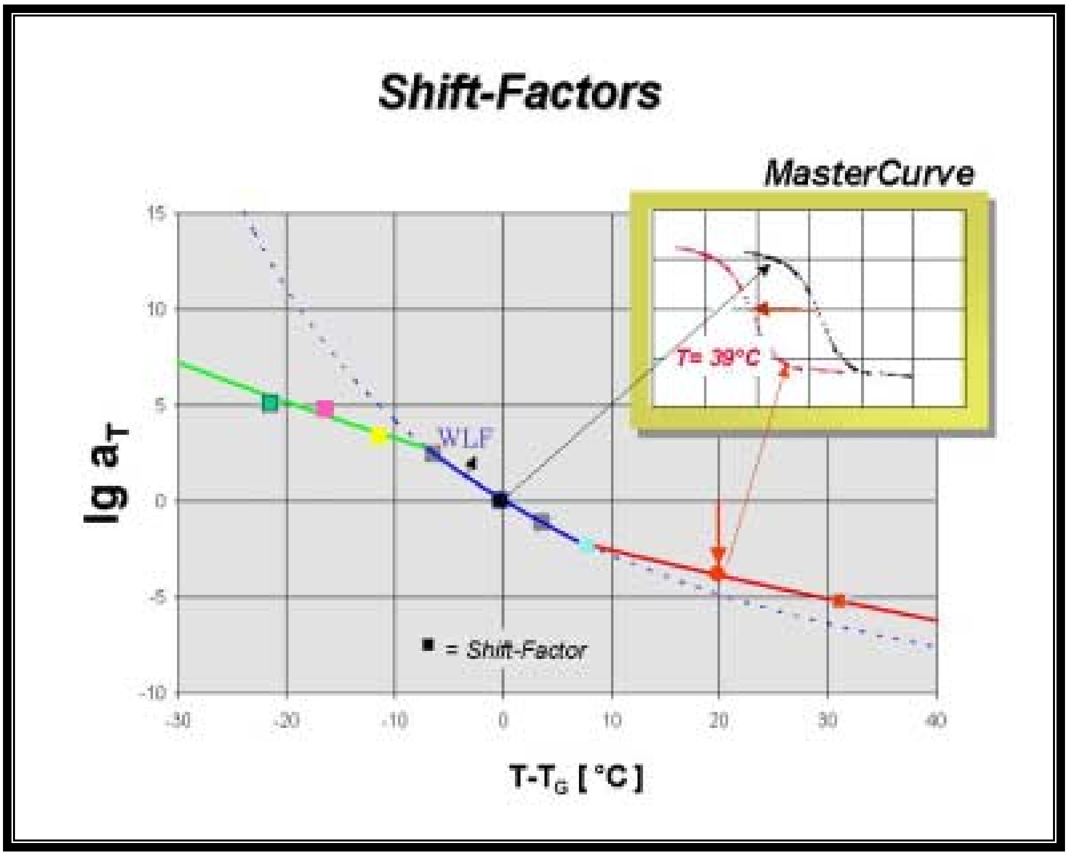

Fig.3.6: Experimental shift-factors are shown. The shift function which represents those values is decomposed into three parts: around the centre of this diagram the shift function is given by the well known WLF- function , while the lower and upper part of this diagram is represented by an Arrhenius – type function. The insert on upper right shows the respective relaxation modulus curve (the black dotted curve represents the master curve, while the red one is shifted).

The shift factors in dependence of temperature shown in ***Fig. 3.6.*** are well represented by the WLF equation in the neighbourhood of the glass-transition temperature T_g only. Therefore an alternative representation is used for the low and high temperature regime. We have used two Arrhenius equations to fit the data in the low as well as in the higher temperature range, respectively. The WLF-shift curve connects the two Arrhenius branches as can be seen from ***Fig. 3.6***. With this approach we are able to fit the experimental shift factors in a broad temperature range within a good quality.

It is clearly seen from Fig.3.6. that for very low and for high temperatures there is a big deviation of the experimental shift factors compared with the prediction of the extrapolated WLF-shift function (see the dotted line). It is important to note that the WLF-equation has been derived under assumptions generally valid in phase transitions. Therefore the WLF-shift function should be applied in the temperature range associated with the glass transition temperature only. In other words: just only in a narrow interval around the neighbourhood of the glass transition temperature T_g , as shown in ***Fig.3.6*** . The functions used in the present analysis for the ***upper*** and ***lower*** temperature range can be derived from the concept of thermally activated processes, which have been expressed in the form of an Arrhenius equation. This type of shift function fits the experimental values of the shift factors in the appropriate temperature ranges very well as can be seen from ***Fig.3.7*** .

3.6 How to fit experimental data

Time-Domain

Using the standard model (generalised Maxwell model of the n'th order) of viscoelasticity for stress relaxation one arrives at:

$$E(t\ ;\ T_g) \ = \ E_\infty + \sum_{i=1}^{N} (E_{i-1} - E_i) \exp(-\frac{t}{\tau_i}) \ , \qquad (1)$$

where E_∞ is the modulus at equilibrium and E_i as well as τ_i are the parameters of the discontinuous relaxation spectra (Prony series). E_N is set equal to E_∞ and E_0 is called the glassy modulus, defined as :

$$E_0 \equiv \lim_{t \longrightarrow 0} E(t;T_g) = E_\infty + \sum_{i=1}^{N} (E_{i-1} - E_i) \quad . \qquad (2)$$

When using N=1, then the above formula (1) takes the following form:

$$E(t\ ;\ T_g) = E_\infty + (E_0 - E_\infty)\exp(-\frac{t}{\tau_1}) \qquad (3)$$

Using (2) in order to eliminate E_∞ in (3) one arrives at

$$E(t\ ;T_g) = E_0[1-e_1]\ .\ \left(1-\exp\left(-\frac{t}{\tau_1}\right)\right), \qquad (4)$$

where we have defined:

$$e_1 \equiv \frac{E_0 - E_\infty}{E_0} \qquad (5)$$

Using formula (4) in order to represent the given master curve one gets the result shown in ***Fig. 3.7***, where we have a comparison of the modulus function with the experimental values of the resulted master curve. The parameters e_1 and τ_1 have been chosen in such a way that a “best fit” to the experimental values could be achieved. Of course the quality of the resulted fit shown is not sufficient, but at small values of time as well as for large times the model function describes the observations rather well. What is not met is the transition range from the glassy to the rubbery state. We may state that the transition according to the used model of the first order is essentially narrower than given by the measurement.

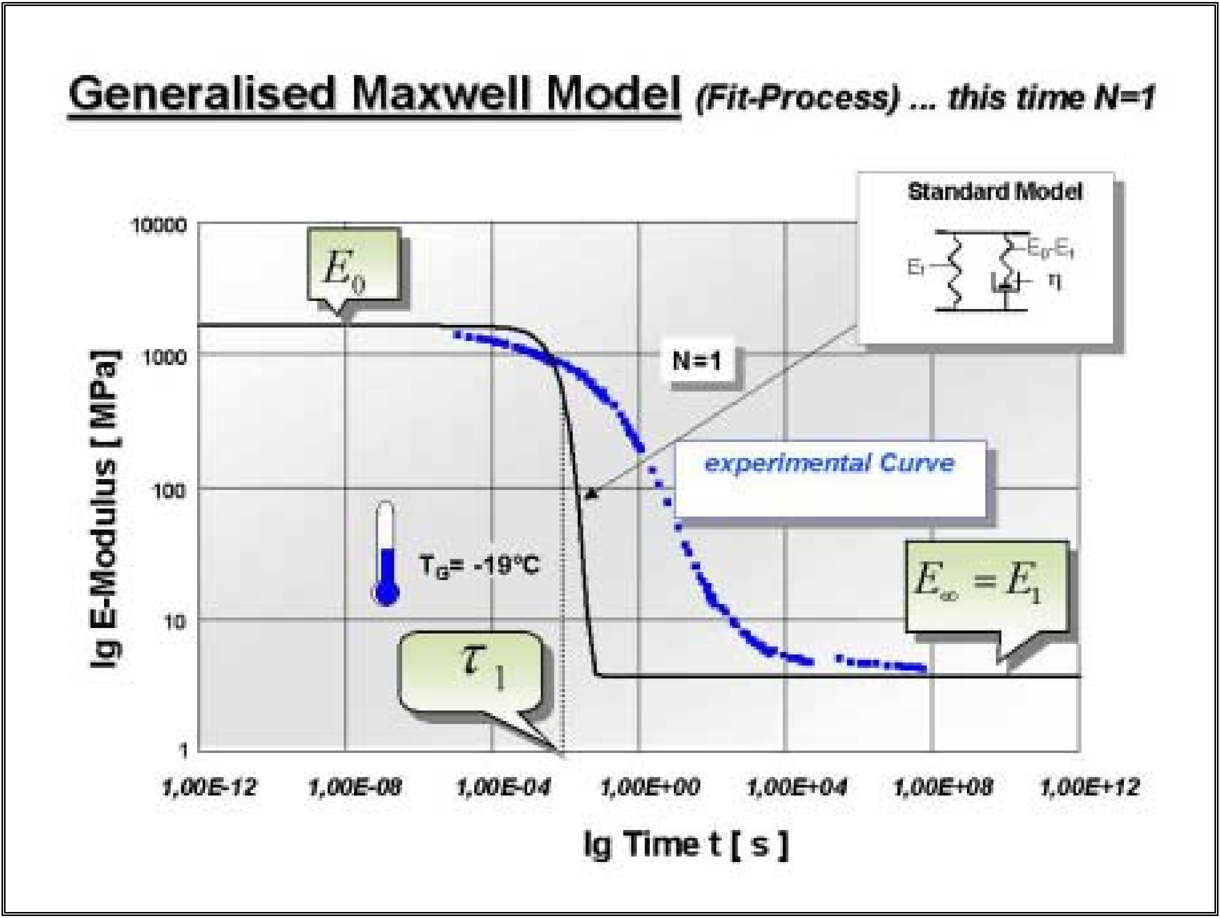

Fig.3.7a: The behavior of the ***standard model*** of visco-elasticity under constant strain: At small times, the modulus possesses a high value (glassy value $\mathbf{E_0}$) and is determined of the sum of both spring rate constants $\mathbf{E_1}$ and $\mathbf{E_0}$**-**$\mathbf{E_1}$. In the long term (large times), the modulus is low and is determined by the spring rate $\mathbf{E_1}$. For small times the effect, of the dash pot is high and therefore the influence of the spring rate $\mathbf{E_0}$**-**$\mathbf{E_1}$ on the level of the modulus is important. In case of $\mathbf{E_0>>E_1}$ there is a drastic transition from high to low modulus at the relaxation time constant τ_1.

In order to describe the transition correctly, it is needed to consider not only one but many Maxwell elements all with different ‘spring rates’ and relaxation time constants. ***Fig.3.7b*** shows the result when a model with three Maxwell elements has been used. Each Maxwell element defines a relaxation time constant and a depth of a ‘transition’ which occurs at the appropriate relaxation time constant. One can imagine that the more transition steps are available the better the ‘generalised Maxwell model’ is able to adopt the given measurement results. ***Fig.3.8*** uses 14 Maxwell elements, therefore we do hardly see any steps in the approximation curve.

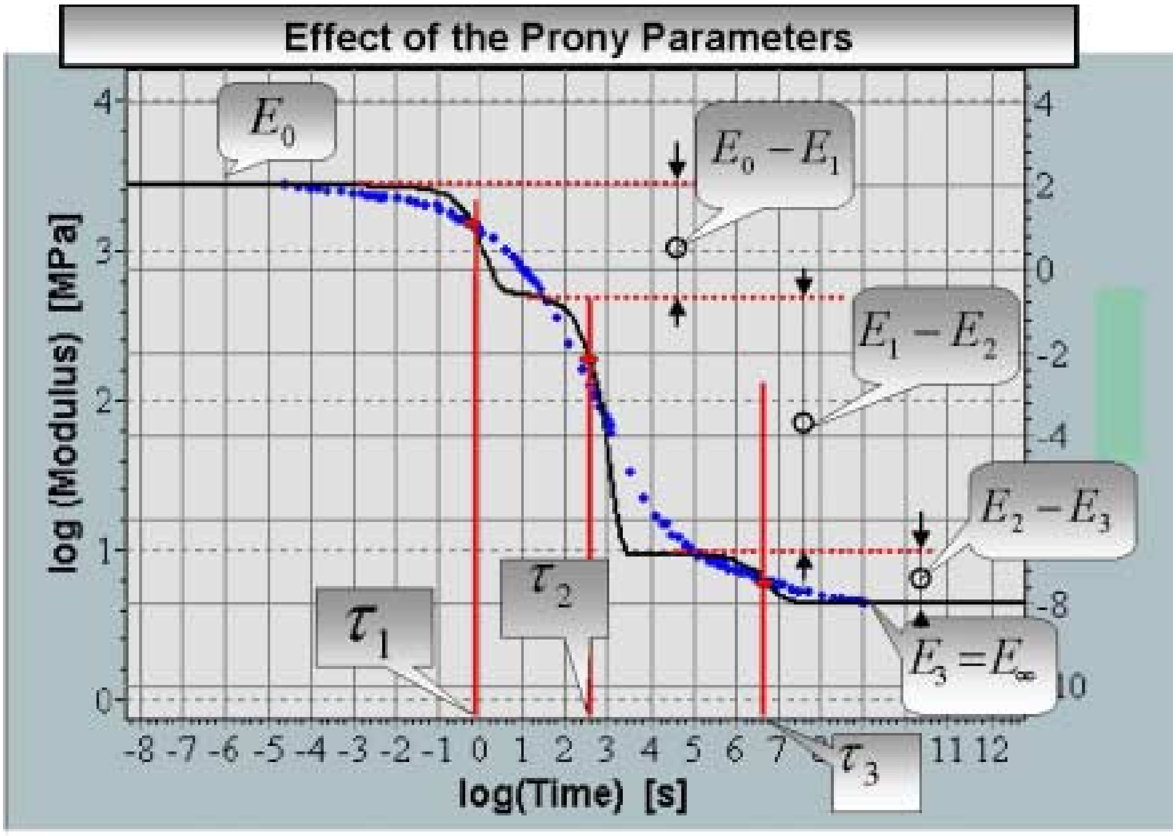

Fig.3.7b: Three steps in the approximated curve are clearly see. They reflect the three Maxwell elements used for the present fitting-model. Those unwanted steps can be avoided if a lot of Maxwell elements are used , as seen in ***Fig.3.8*** .

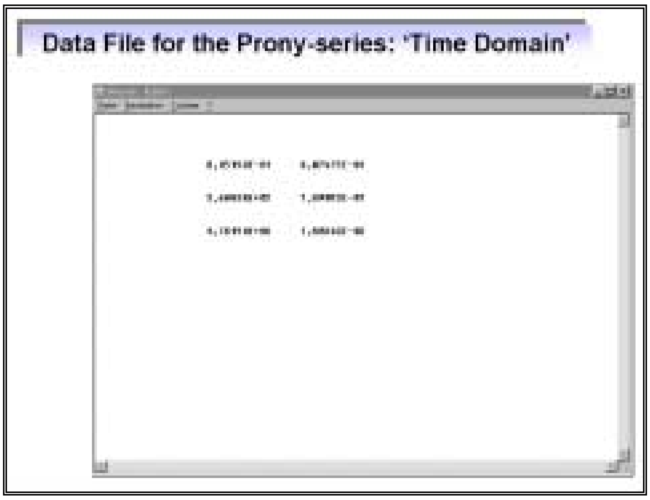

Data File for the Prony-series: 'Time Domain'

Fig.3.7c: List of PRONY-parameters according to the used Model of the third order.

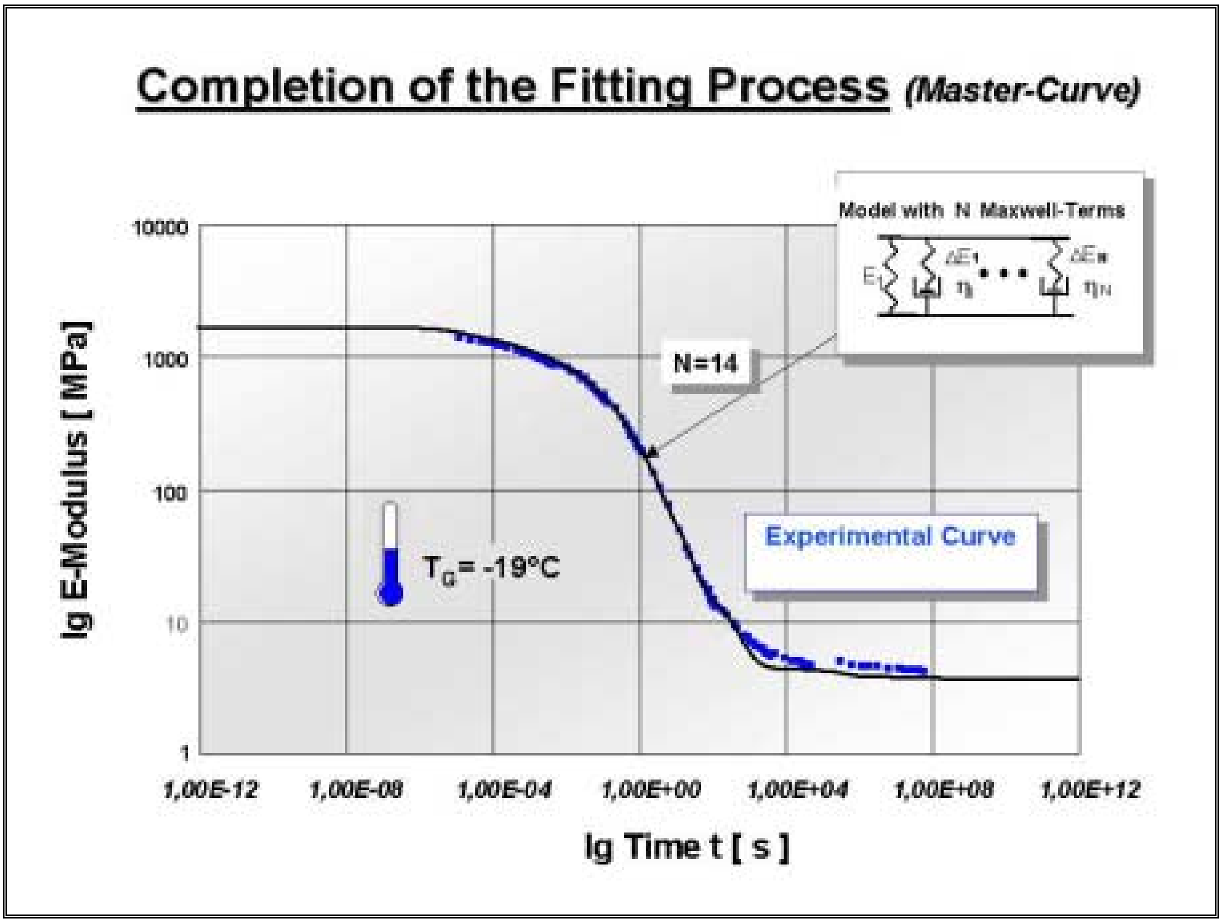

Fig.3.8: Adding further Maxwell elements to the constitutive model increases the ability to get a better fit to the experimental values of the master curve. This time it turns out that 14 Maxwell elements may be sufficient .

If in general N Maxwell elements have been used the formula which describes the experimental values of the master curve can be written as follows (see also equation (1) and (2)):

$$E(t\ ;\ T_g) = E_0\left[1-\sum_{i=1}^{N} e_i\left(1-\exp\left(-\tfrac{t}{\tau_i}\right)\right)\right] \quad , \qquad (6)$$

where $e_i = (E_{i-1} - E_i)/E_0 = (\Delta E)_i / E_0$ has been used.

The parameters E_0 , e_i and τ_i have to be chosen in such a way that a “best-fit” may be achieved (see for example ***Fig 3.8***).

In order to get a modulus–time characteristic for other than reference temperature we have to use the information provided by the shift-factors. As indicated earlier it might be suitable to split up the shift function into three parts. ***Fig.3.9*** and equation (8) show the mathematical form of those distinct branches of shift function. Thus the modulus-time-temperature function may be described as:

$$E(\ t\ ;\ T\ ) = E_0\left[1-\sum_{i=1}^{N} e_i\left(1-\exp\left(-\frac{t}{\tau_i a_T}\right)\right)\right], \qquad (7)$$

where

$$\lg(a_T)^{+1} = \begin{array}{lll} \left\langle -\dfrac{C_1(T_c^U - T_g)}{C_2 + T_c^U - T_g} - \dfrac{MA_E^U}{RT_c^U}\dfrac{(T-T_g)+(T_g-T_c^U)}{T_g+(T-T_g)} \right. & & 0 \le T \ge T_c^U \\ \left\langle -\dfrac{C_1(T-T_g)}{C_2+T-T_g} \right. & & T_c^U \le T \le T_c^O \\ \left\langle -\dfrac{C_1(T_c^O - T_g)}{C_2 + T_c^O - T_g} - \dfrac{MA_E^O}{RT_c^O}\dfrac{(T-T_g)+(T_g-T_c^O)}{T_g+(T-T_g)} \right. & & T_c^O \le T \le \infty \end{array} \qquad (8)$$

is used.

Thus a set of parameters have been defined which are able to reflect the thermo-visco-elastic behavior of a given rubbery material. They are:

➔ Prony series : pairs of $\langle e_i \,|\, \tau_i \rangle \ i = 1,\dots,N$

➔ shift parameters: $C_1 \ , \ C_2 \ , \ T_g \ , \ T_c^U \ , \ T_c^O \ , \ A_E^U \ , \ A_E^O$ (9)

where the first and the second one of the set given in the last line are non-adjustable parameters, while **R** is a universal number and **M** is a numeric value (where **R** gives the universal gas constant and **M**=$\lg(e) = 0.43429$).

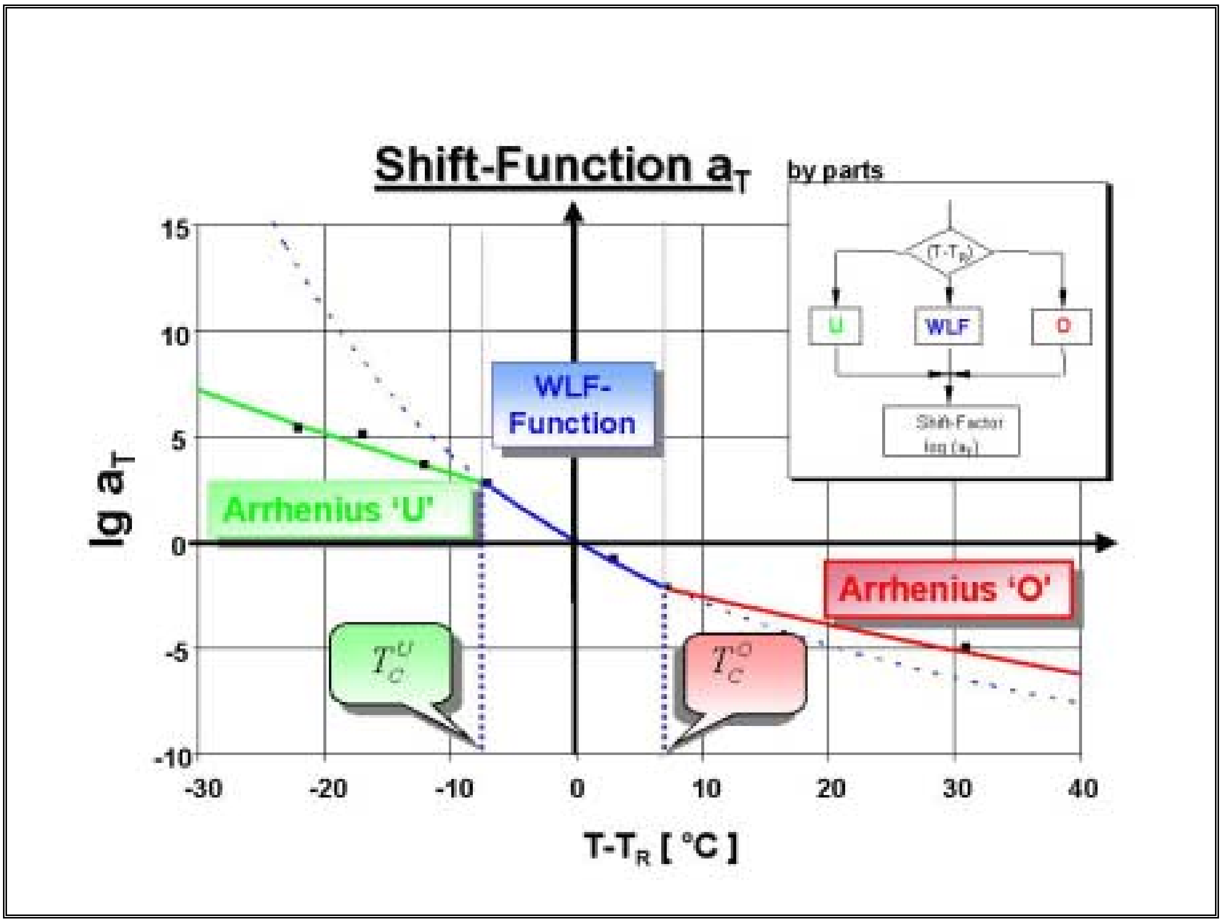

Fig.3.9: The shift-factors are described by three different shift functions (see also formula (8)). The reference temperature T_R has been identified with the glass transition temperature T_g. The indicated characteristic temperatures T_c^U *and* T_c^O in the plot represent the limits of the validity of the various branches. The WLF-function, valid for temperatures in the neighbourhood of T_g, possesses the form: $C_1(T-T_g)/(C_2+T-T_g)$. It is important to note that C_1 *and* C_2 are considered as non - adjustable parameters rather they are used as universal constants and possess the following numerical values: $C_1=-17.44$; $C_2=51.6$.

In a somewhat more general loading case, than already described by (7), we may prescribe the strain **ε** in a uni-axial loading mode as an arbitrary function of time. Then we end up with the following constitutive equations using once again the already determined constitutive parameters given (9):

$$\sigma \ = E_0\left[\varepsilon(t) - \sum_{i=1}^{N} e_i \zeta_i\right] \tag{10$_1$}$$

$$\dot{\zeta}_i = -\frac{1}{\tau_i}\left(\zeta_i - \varepsilon(t)\right) \quad i = 1, \cdots, N \text{ ,} \tag{10$_2$}$$

where ζ $_i$ can be considered as internal variables (internal “strains” !). All the other parameters are already known from the above mentioned evaluation of the simple stress relaxation experiment. By solving the given N ordinary differential equations of the first order in (10)$_2$ we may determine the functions ζ $_i$ at time *t* and may then the resulted values insert into (10)$_1$ in an incremental manner which gives the $\langle\sigma|\varepsilon\rangle$ characteristics of the material in question in dependence of a predefined strain function. Thus we may be able to predict transient responses when the material is subjected to any uniaxial loading condition (sinusoidal varying strain may be just one example, another may be step-like constant strain loading – leading to stress relaxation).

Frequency Domain

In case a test is made in the frequency domain one gets the storage modulus as well as the loss modulus. In the following we shall exclusively consider the storage modulus as an example. The procedure valid for the loss modulus is more or less the same as for the storage modulus. The ideal-elastic solid has a modulus which is time independent. During dynamic testing of an ideal-elastic body, the prescribed strain may be represented by the function

$$\varepsilon(t) = \varepsilon_0 \sin(\omega t),$$

which yields the stress as

$$\sigma(t) = \varepsilon_0 E \sin(\omega t). \tag{11}$$

For the viscoelastic material, both the strain and the stress again vary sinusoidally, but the strain lags behind the stress, as shown in ***Fig.3.10***. Mathematically we have,

$$\varepsilon(t) = \varepsilon_0 \sin(\omega t)$$

$$\sigma(t) = \sigma_0 \sin(\omega t + \delta), \tag{12}$$

where ω is the angular frequency, and δ is the phase lag. From trigonometric relations we have:

$$\sigma = (\sigma_0 \cos\delta)\sin\omega t + (\sigma_0 \sin\delta)\cos\omega t\,, \tag{13}$$

so the stress can be decomposed into components (1) : $\sigma_0 \cos\delta$, which is in phase with the strain and (2): $\sigma_0 \sin\delta$, which is out of phase with the strain. The constitutive equation for linear viscoeasticity under uniaxial straining is based on the fact that the effects of sequential changes in strain are additive [1], therefore :

$$\sigma(t) = \int_{-\infty}^{t} E(t - t')\,\dot{\varepsilon}(t')\,dt' \,. \tag{14}$$

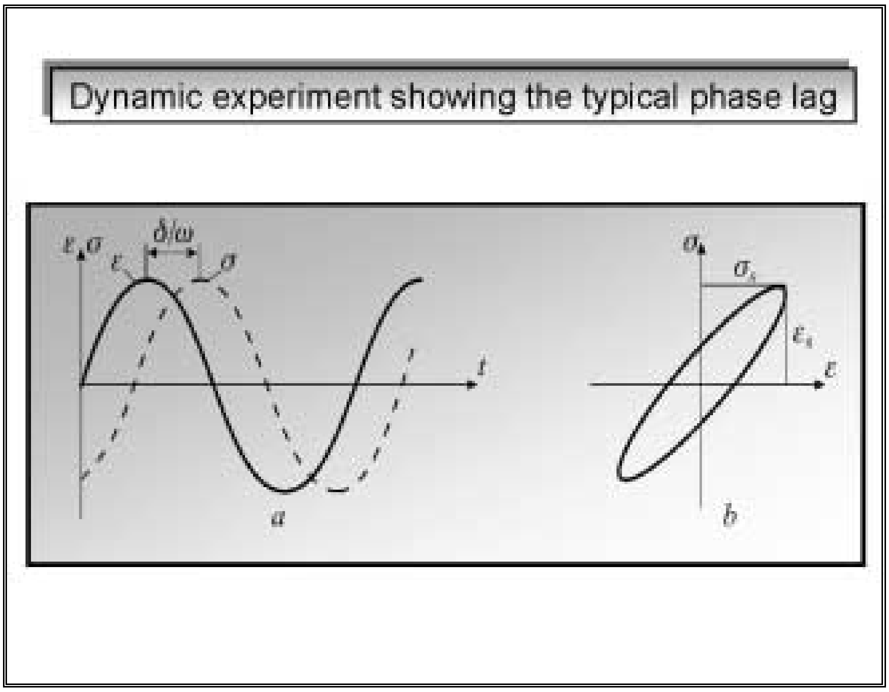

Fig. 3.10: Strain and the resulting stress in a dynamical experiment, where the strain is prescribed in a sinusodial mode. The given stationary state shows clearly a lag between stress and strain ***(a).*** The diagram on the right shows ***(b)*** a plot where the stress is given in dependence of strain (a hystersis appears as an other indication of viscoelastic behavior).

Using the given strain-rate function and integrating formula (14) one arrives at:

$$\sigma(t) = \varepsilon_0 \left[E' \sin \omega t + E'' \cos \omega t \right], \qquad (15)$$

where E' is the so called storage modulus, while E'' represents the loss modulus. The nomenclature of complex numbers is also commonly used in this respect, but we do not use them here.

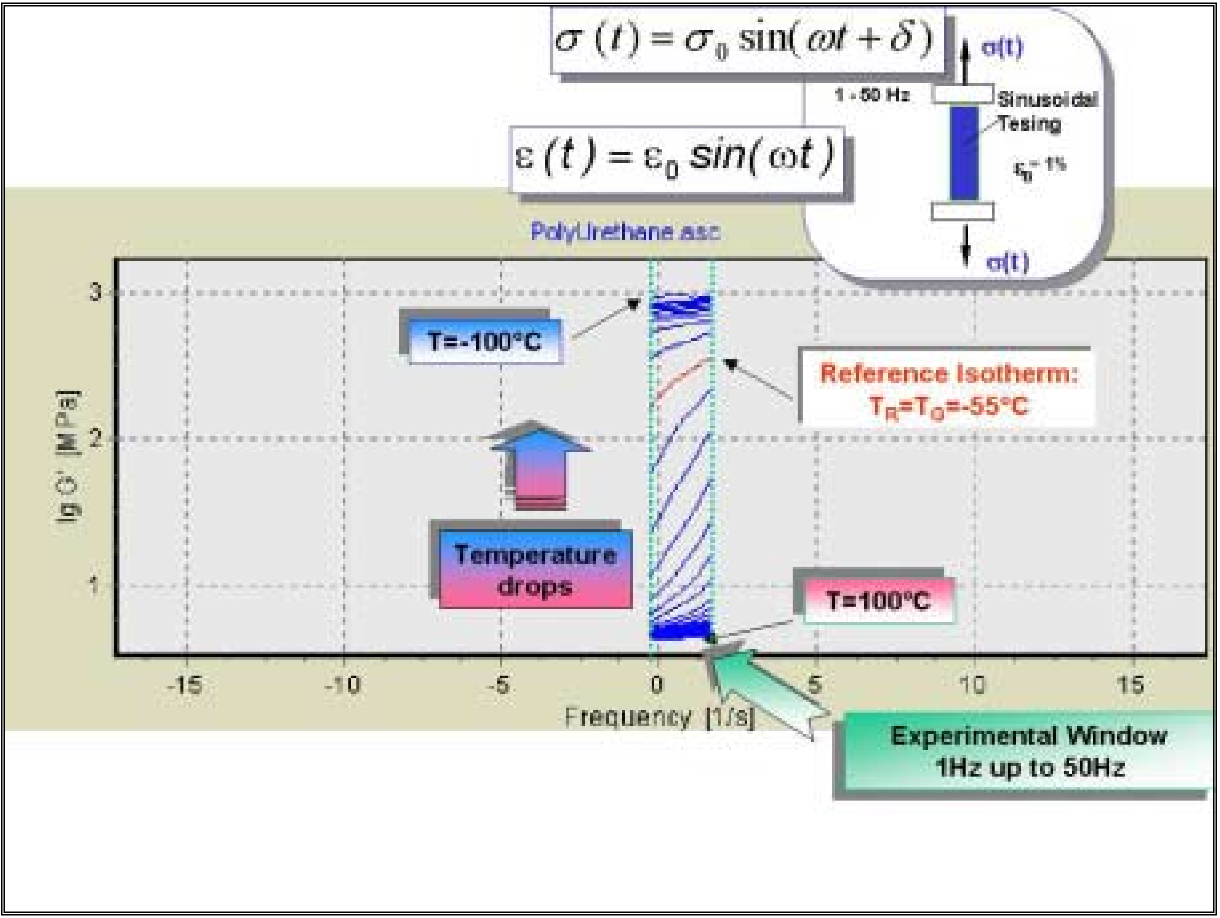

Fig.3.11: Storage modulus G' of a typical thermoplastic polyurethane grade as function of imposed frequency for various constant temperatures. Temperature is parameter of the given set of storage modulus isotherms. The set of various temperature starts with T=-100°C and ends up with +100°C (from top to bottom; 40 isotherms are measured, equidistantly distributed). 10 individual frequencies equidistantly distributed on the logarithmic scale of the 'experimental window' have been applied as imposed frequency. It turns out that the chosen reference temperature is identical to the given glass transition temperature T_G=-55°C.

For example storage modulus G' (note that a well known relation exists between G' and E', that is to say they can be expressed in terms of each other) are found to depend on the frequency of vibration, which can be shown when measuring a typical thermoplastic polyurethane grade with a Shore-Hardness of about '85 Shore A' and a glass transition temperature of about –55°C, as given in ***Fig. 5.*** As the imposed frequency is raised, the storage modulus increases, the more the temperature approaches the characteristic reference temperature T_g coming from the higher temperature end. When going beyond T_g and decreasing the temperature further the increase in storage modulus decreases and eventually at very low temperature vanishes altogether.

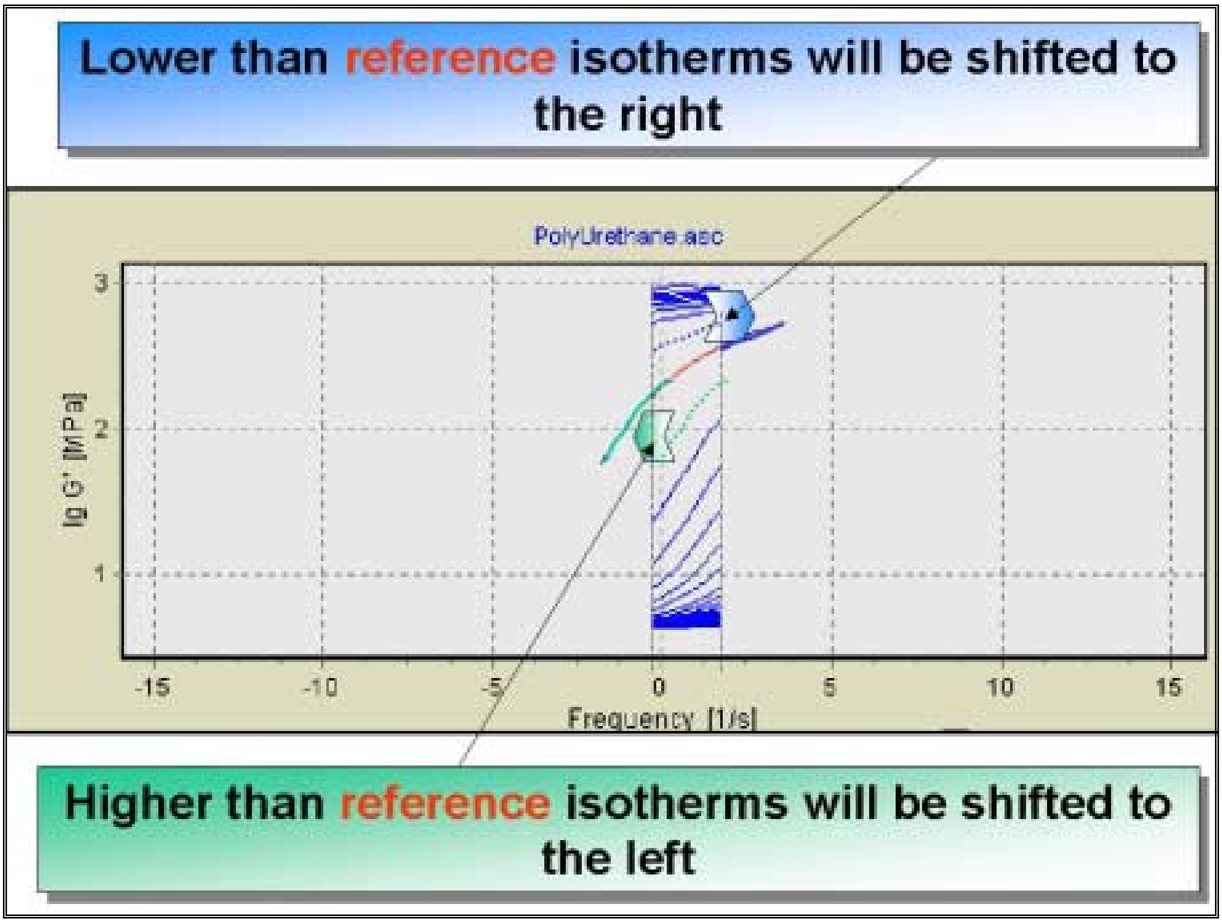

Fig.3.12: Starting shifting procedure: Isotherms with temperature lower than the reference temperature shall be shifted to the right (... that is the opposite direction as in case of 'time domain' curves) All the other isotherms, that is to say, higher than reference temperature, will be shifted to the left (once again this is the opposite direction as in case of time dependent modulus curves, see earlier section ...).

It turns out that a measurement at one temperature can be applied at another, similar like already seen previously in the 'time domain'. A temperature change is completely equivalent to a change in inverse frequency. Thus measurements can be taken over a limited frequency range at many different temperatures, as shown in ***Fig. 3.11***. They are then superimposed by lateral shifts along the logarithmic frequency axis to construct a "master-curve", representing the expected response over an extremely wide frequency range at the chosen reference temperature (see ***Fig. 3.12/3.13***).

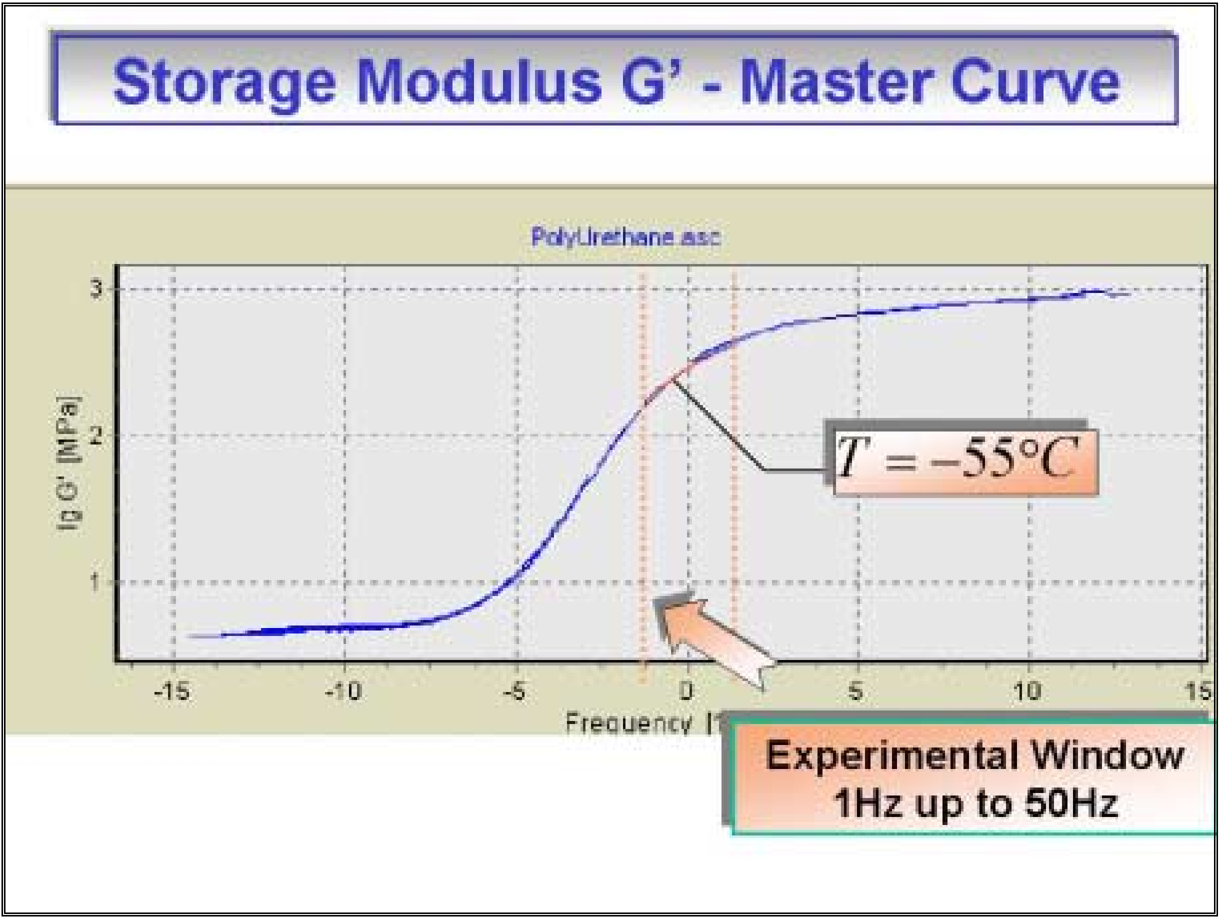

Fig.3.13: Completion of the shifting procedure: The graph shows the master curve, build up from the individual isotherms given in ***Fig.3.11*** and ***Fig.3.12*** by shifting the curves relative to the chosen reference isotherm. All the isotherms with temperature lower than the temperature of the reference isotherm have been shifted to the right, while the remaining ones were shifted to the left. The effective shifting has been done according to the shift-function given in formula ***(16).*** Compare also this formula with formula ***(8)*** , which has been applied in the 'time domain', and note that the terms in both of the formulae are identical with the exception that the sign of the function has changed from plus to minus sign.

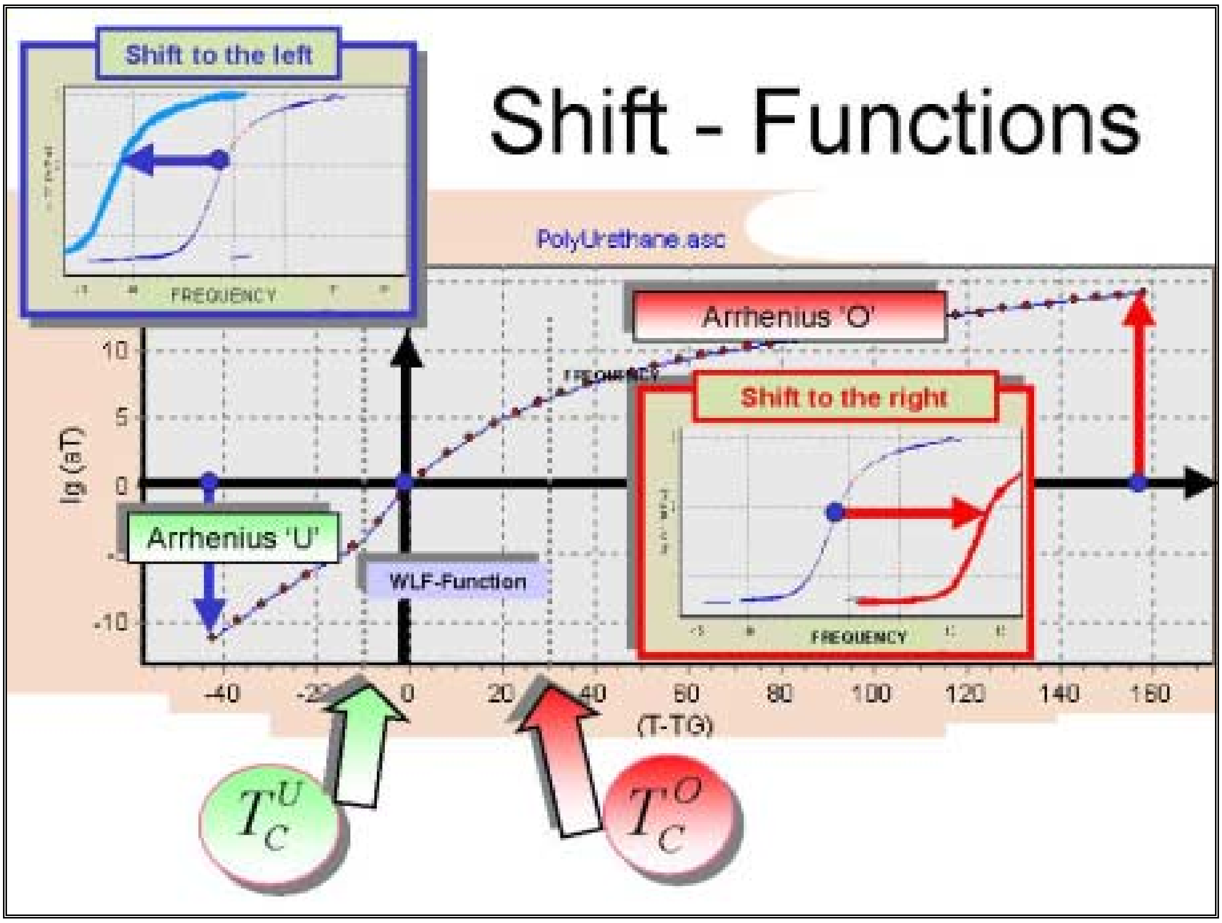

Fig.3.14: The plot in the ***(lg(a$_T$),T-T$_G$)*** - diagram shows the shift-factors as well as the shift-functions used in getting the master curve shown in ***Fig.3.13***. Also shown is the effect of shifting on the master curve by choosing two different temperatures, namely T=-100°C (see upper left insert) where the master curve is shifted roughly 10 orders of magnitude to the left, while on the lower right insert one observes a shift of the master curve approx. 15 orders to the right in order to represent the effect of a high temperature (+100°C). Compare also this plot with the one shown in ***Fig.3.9*** and note that they are mutually mirror - images

The shift functions applied in ***Fig.3.13*** and shown in ***Fig.3.14*** are represented by the following formula:

$$\lg\left(a_T\right)^{-1} = \begin{cases} -\dfrac{C_1(T_c^U - T_g)}{C_2 + T_c^U - T_g} - \dfrac{MA_E^U}{RT_c^U}\dfrac{\left(T - T_g\right) + \left(T_g - T_c^U\right)}{T_g + \left(T - T_g\right)} & 0 \le T \ge T_c^U \\ -\dfrac{C_1\left(T - T_g\right)}{C_2 + T - T_g} & T_c^U \le T \le T_c^O \\ -\dfrac{C_1\left(T_c^O - T_g\right)}{C_2 + T_c^O - T_g} - \dfrac{MA_E^O}{RT_c^O}\dfrac{\left(T - T_g\right) + \left(T_g - T_c^O\right)}{T_g + \left(T - T_g\right)} & T_c^O \le T \le \infty \end{cases} \tag{16}$$

Note that this formula is identical with formula (8) with the exception of the sign of lg(a_T). While the sign was positive for the 'time-domain' shift-function given in (8) the sign is now negative (see above formula (16)), that is to say, the original function given in (8) may be considered as the mirror-image of (16) where the abscissa is the axis of symmetry.

Applying the constitutive description of the generalised Maxwell model on equation (12) – (15) we may describe the storage modulus with respect to the discrete relaxation spectra (Prony series) as follows (see ***Fig.3.15) .***

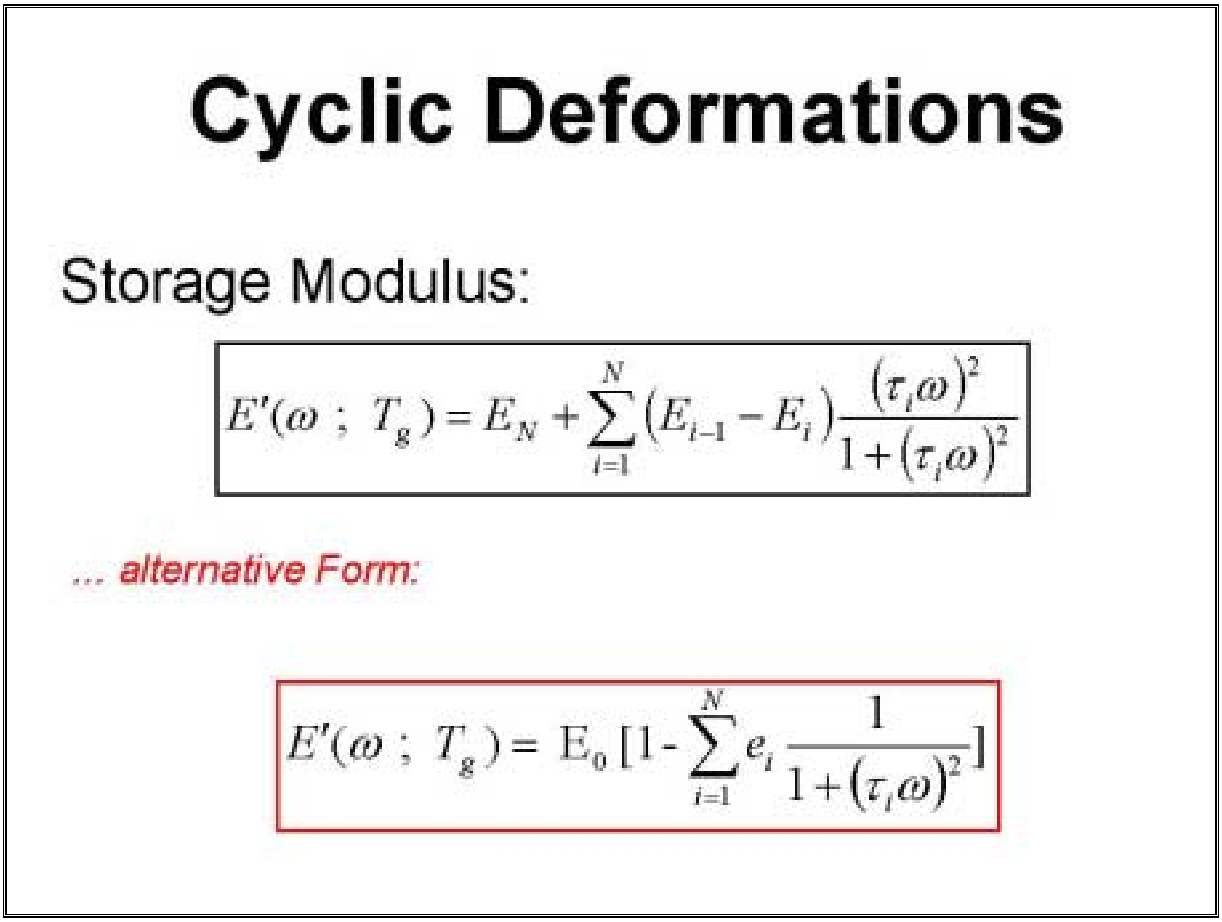

Cyclic Deformations

Storage Modulus:

$$E'(\omega \; ; \; T_g) = E_N + \sum_{i=1}^{N} \left(E_{i-1} - E_i\right) \frac{\left(\tau_i \omega\right)^2}{1+\left(\tau_i \omega\right)^2}$$

... alternative Form:

$$E'(\omega \; ; \; T_g) = \mathrm{E}_0 \,[1 - \sum_{i=1}^{N} e_i \frac{1}{1+\left(\tau_i \omega\right)^2}]$$

Fig. 3.15: Storage modulus formulae are shown and described in terms of a line spectra (Prony series). For the definitions of E_0 and e_i see also formulae (2) and (5), respectively.

.

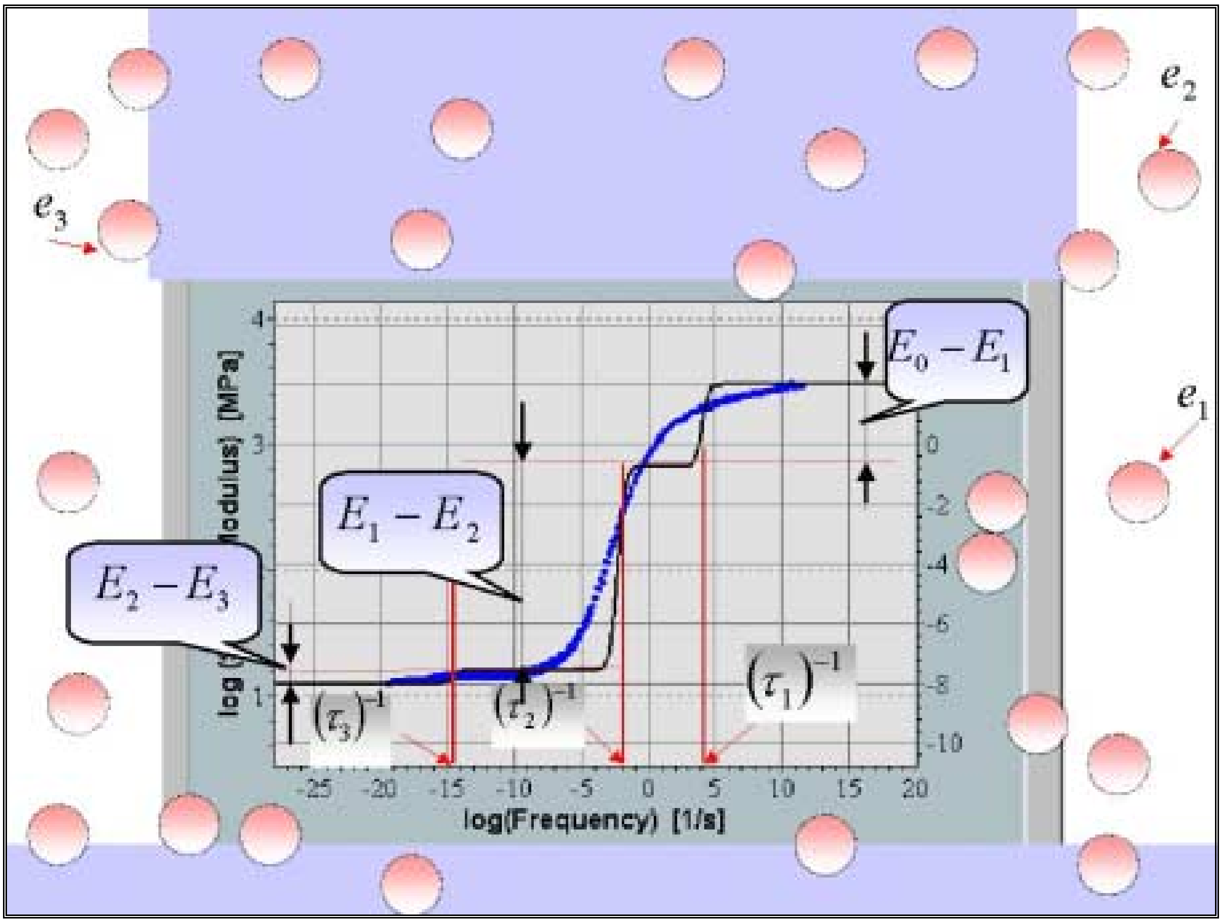

Fig.3.16: Fit by a model of the third order (equivalent to three relaxation time constants:

$$\tau_3 = 3.3981 \cdot 10^{+14}\,\text{sec} \;;\; \tau_2 = 77.4453\,\text{sec} \;;\; \tau_1 = 6.91088 \cdot 10^{-5}\,\text{sec}$$

The red balls found in this figure will just say, that one need more than three relaxation time constants to get a well representation of the experimental master curve.

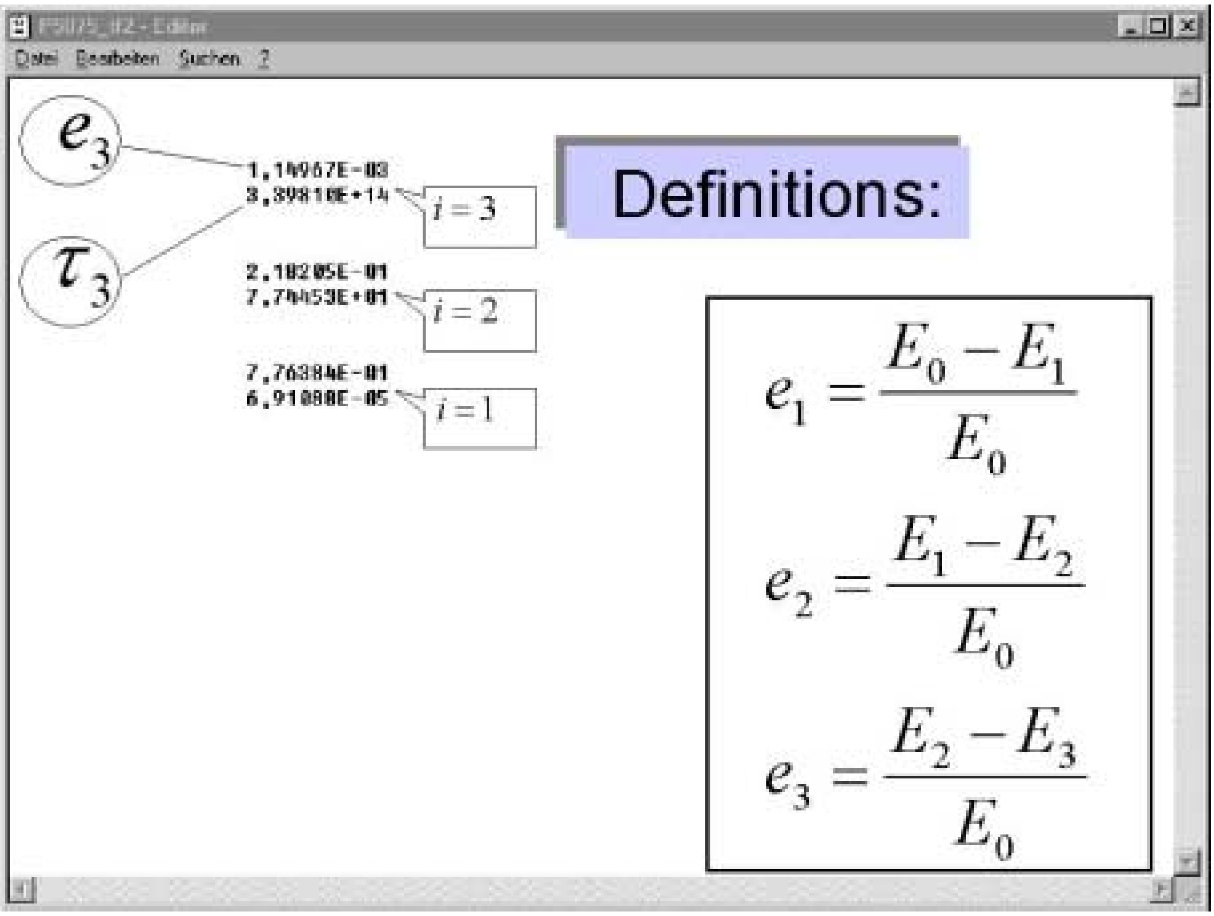

```
1,14967E-03
3,89810E+14

2,18205E-01
7,74453E+01

7,76384E-01
6,91080E-05
```

Definitions:

$$e_1 = \frac{E_0 - E_1}{E_0}$$

$$e_2 = \frac{E_1 - E_2}{E_0}$$

$$e_3 = \frac{E_2 - E_3}{E_0}$$

Fig.3.17: List of relaxation strength and relaxation time constants, respectively. (Prony-series). Order of model is N=3. See also ***Fig. 3.15.***

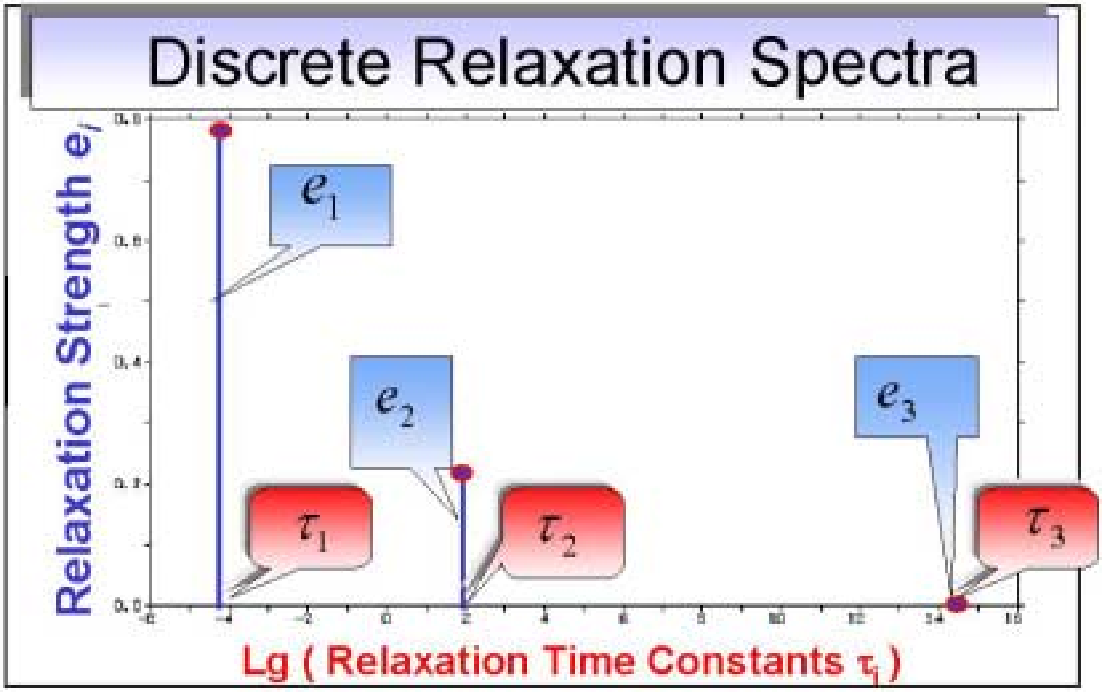

Fig.3.18*:*Relaxation Spectra (line spectra: N=3): *Relaxation strength* versus *lg(relaxation time)*

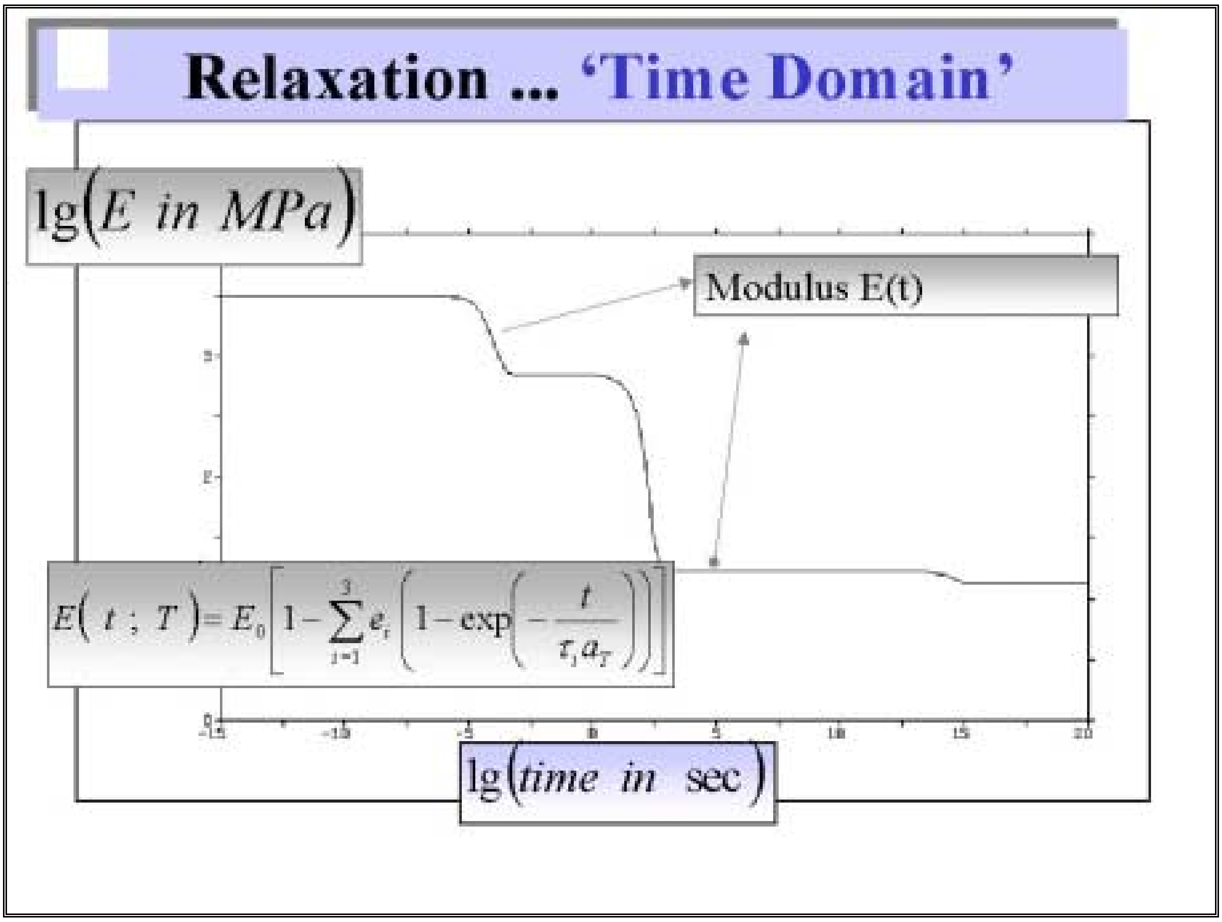

Fig.3.19: Prediction of the transient behavior using the Prony parameters determined already in the frequency domain (see above). According to the model used (three Maxwell terms appear), there are three distinct transitions shown (three steps of different depth !). This behavior results when a step-like (suddenly loading) strain ε_0 is imposed and the set of equations (10) are used or equivalently when applied above indicated relaxation function. Here a_T is set equal to 1, that is to say the reference temperature is used.

4. Applying ViscoShift and ViscoData

4.1. Tutorial

Applying this software package is illustrated by means of examples, which the user can follow along at his own computer screen. An appropriate Tutorial/Handbook is available on request***(additionally a DEMO-Version of ViscoData can be downloaded from the INTERNET: http://www.ViscoData.de).***

5) Concluding remarks

The greatest value of the software system presented in this handbook is a quick and liable determination of the parameters of a discrete relaxation spectra of rubbers and plastics (called a Prony-series). Although the method used are generally restricted to non-cristalline polymers, applications to cristalline materials is possible within restricted temperature domains.

Last but not least it is needless to say that the concept of a Prony series is also applicable to other than polymer materials. For example metals, ceramics, glasses etc. are also candidates for the proposed concept, because they are as well visco-elastic materials in nature. For those materials usually the relaxation spectra is narrower (only few relaxation time constants are needed to represent the viscoelastic behavior of those materials) compared with elastomers. But never the less visco-elastic properties may be also important, especially under higher temperatures.

6) References

[1] Ferry, J.D., 1980, Viscoelastic Properties of Polymers, 3rd ed. New York: Wiley.
[2] Tobolsky, A.V. 1960. Properties and Structures of Polymers. New York: Rheinhold
[3] Ward, I.M. 1983. Mechanical Properties of Solid Polymers, 2nd. Ed. New York: Wiley
[4] Flory, P.J. 1953, Principles of Polymer Chemistry. New York: Cornell University Press
[5] L.R.G. Treloar, The Physics of Rubber Elasticity, 3rd ed., Oxford University Press,London,1975
[6] Williams, Landel, Ferry, 1955. J. Am. Chem. Soc., 77: 3701.
[7] Ajroldi and co-workers, report available by AUSIMONT, Italy.
[8] MARC – European - User - Meeting, helt in Duesseldorf, Germany, 1996:
"Simulation of Time and Temperature Effects of Elastomeric Materials"
[9] M. Achenbach, G. Streit, 2001, Gummi Fasern Kunststoffe (GAK) 54, 164-178